$J_{5,6}$ = 8.1 Hz), 6.26 (t, 1, H-1', $J_{1',2'}$ = 7.5 Hz), 7.98 (d, 1, H-6); ^{13}C NMR (Me_2SO-d_6) δ 41.25 (C-2'), 58.98 (C-4'), 60.11 (C-1', ^1J = 163.4 Hz), 63.47 (C-5'), 73.44 (C-3'), 102.13 (C-5, J = 175.9 Hz), 141.35 (C-6, J = 180.8 Hz), 150.62 (C-2), 162.74 (C-4). Anal. ($C_9H_{12}N_4O_2S$) C, H, N, S.

Compound 4α (262 mg) was deprotected in a similar manner as described for 4β to provide 11 (120 mg, 90%): mp 190–192 °C; TLC (9:1 $CHCl_3$–MeOH) R_f 0.30; MS z/e 245 $(M + 1)^+$; UV λ_{max} (pH 1) 266 (9.24), (pH 7) 266 (9.52), (pH 13) 265 (8.72); ^{1}H NMR (Me_2SO-d_6) δ 2.04 (dt, 1, H-2'a, $J_{2'a,2'b}$ = 14.3 Hz, $J_{1',2'a}$ = $J_{2'a,3'}$ = 3.3 Hz), 2.50 (ddd, 1, H-2'b, $J_{1',2'b}$ = 8.3 Hz, $J_{2'b,3'}$ = 4.6 Hz), 3.34 (m, 1, H-5'a, $J_{5'a,5'b}$ = 11.0 Hz, $J_{4',5'a}$ = 6.7 Hz), 3.44 (m, 1, H-5'b, $J_{4',5'b}$ = 6.7 Hz), 3.55 (t of d, 1, H-4', $J_{3',4'}$ = 2.7 Hz), 4.32 (m, 1, H-3'), 5.05 (br s, 1, OH), 5.49 (br s, 1, OH), 5.65 (d, 1, H-5, J = 8.1 Hz), 6.14 (dd, 1, H-1'), 8.26 (d, 1, H-6), 11.24 (br s, 1, H-3); ^{13}C NMR (Me_2SO-d_6) δ 42.16 (C-2'), 60.01 (C-4'), 60.96 (C-1', ^1J = 161.5 Hz), 63.57 (C-5'), 74.14 (C-3'), 101.16 (C-5, $^1J_{C,H}$ = 175.2 Hz), 142.92 (C-6, J_{CH} = 181.9 Hz), 150.7 (C-2), 162.98 (C-4). Anal. ($C_9H_{12}N_4O_2S$) C, H, N, S.

4'-Thiothymidine (10) and 1-(2-Deoxy-4-thio-α-D-*erythro*-pentofuranosyl)thymine (12). A solution of 5β (150 mg, 0.30 mmol) in anhydrous MeOH (30 mL) was stirred at room temperature with a freshly prepared solution of sodium methoxide (32.5 mg, 0.60 mmol) in MeOH (5 mL). A TLC aliquot (3 h, $CHCl_3$–MeOH, 95:5) showed complete consumption of starting material. The solution was rendered neutral with Dowex 50W-X8 (H^+) ion-exchange resin, and the resin was filtered off, with MeOH washing. The filtrates were combined and evaporated to dryness, and methyl p-toluate was removed at 50 °C/0.01 Torr. Crystallization of the residue from absolute EtOH gave pure 10 (61 mg, 78%): mp 213–215 °C; TLC (9:1 $CHCl_3$–MeOH) R_f 0.40; MS z/e 258 (M + 1); UV λ_{max} (pH 1) 272 (10.3), (pH 7) 272 (10.2), (pH 13) 271 (10.3); ^{1}H NMR (Me_2SO-d_6) δ 1.80 (d, 3, 5-CH_3, $J_{6,5\text{-}CH_3}$ = 1.1 Hz), 2.14 and 2.19 (m, 2, H-2'a, H-2'b, $J_{2'a,2'b}$ = 13.1 Hz, $J_{1',2'a}$ = 6.7 Hz, $J_{1',2'b}$ = 8.5 Hz, $J_{2'a,3'}$ = 3.4 Hz, $J_{2'b,3'}$ = 3.9 Hz), 3.28 (t of d, 1, H-4', $J_{3',4'}$ = 2.2 Hz), 3.52–3.67 (m, 2, H-5'), 4.38 (br s, 1, H-3'), 5.16 (br t, 1, 5'-OH), 5.24 (d, 1, 3'-OH, J = 3.7 Hz), 6.30 (dd, 1, H-1'), 7.81 (br q, 1, H-6), 11.32 (br s, 1, H-3); ^{13}C NMR (Me_2SO-d_6) δ 12.14 (5-CH_3), 40.98 (C-2'), 59.01 (C-4'), 59.93 (C-1', $J_{C,H}$ = 161.7), 63.51 (C-5'), 73.40 (C-3'), 109.82 (C-5), 136.70 (C-6, $^1J_{C,H}$ = 179.0 Hz), 150.60 (C-2), 163.37 (C-4). Anal. ($C_{10}H_{13}N_2O_4S$) C, H, N, S. H: calcd, 5.09; found, 5.56.

Compound 5α (100 mg, 0.20 mmol) was deprotected in a manner similar to that described for 5β to provide 12 (42 mg, 80% yield) (mp 205–207 °C): TLC (9:1 $CHCl_3$–MeOH) R_f 0.40; MS z/e 258 $(M + 1)^+$; UV λ_{max} (pH 1) 271 (10.5), (pH 7) 271 (10.5), (pH 13) 271 (8.64); ^{1}H NMR (Me_2SO-d_6) δ 1.80 (s, 1, 5-CH_3), 2.05 (d of t, 1, H-2'a, $J_{2'a,2'b}$ = 1.40 Hz, $J_{1',2'a}$ = $J_{2'a,3'}$ = 4.4 Hz), 2.49 (ddd, 1, H-2'b, $J_{1',2'b}$ = 8.2 Hz, $J_{2'b,3'}$ = 4.9 Hz), 3.33–3.38 (m, 1, H-5'a), 3.48–3.60 (m, 2, H-4', H-5'b), 4.26 (m, 1, H-3', $J_{3',4'}$ = 3.0 Hz), 4.99 (br s, 1, 5'-OH), 5.48 (br s, 1, 3'-OH), 6.16 (dd, 1, H-1'), 8.11 (s, 1, H-6), 11.24 (br s, 1, H-3); ^{13}C NMR (Me_2SO-d_6) δ 12.26 (C-5 CH_3), 42.03 (C-2'), 59.53 (C-4'), 59.77 (C-1', $^1J_{C,H}$ = 161.6 Hz), 63.57 (C-5'), 74.05 (C-3'), 108.94 (C-5), 138.28 (C-6, $J_{C,H}$ = 179.6 Hz), 150.62 (C-2), 163.47 (C-4). Anal. ($C_{10}H_{13}N_2O_4S$) C, H, N, S. H: calcd, 5.09; found, 5.54.

Acknowledgment. This investigation was supported by the National Cancer Institute, National Institutes of Health, DHHS, Grant P01 CA34200. We are indebted to Mrs. Sarah Jo Clayton, Mr. T. E. Gillespie, and Mrs. Jackie Truss of the Organic Chemistry Department for large-scale preparation of intermediates, to Dr. W. C. Coburn, Mr. M. Kirk, Mrs. Christine Richards, and Ms. M. D. Ochs for spectral data, to Dr. L. L. Bennett, Jr., and Mrs. Doris Adamson for cytotoxicity evaluations, and to Dr. W. M. Shannon and Ms. G. Arnett for antiviral evaluations.

Registry No. β-1, 24707-95-7; β-2, 68660-42-4; α-3, 134111-36-7; β-3, 134111-26-5; α-4, 134111-37-8; β-4, 134111-27-6; α-5, 134111-38-9; β-5, 134111-28-7; α-6, 134111-39-0; β-6, 134111-29-8; α-7, 134111-40-3; β-7, 134111-30-1; 8, 134111-31-2; 9, 134111-32-3; 10, 134111-33-4; 11, 134111-34-5; 12, 134111-35-6; uracil, 66-22-8; thymine, 65-71-4; cytosine, 71-30-7.

Modeling Study of the Structure of the Macromolecular Antitumor Antibiotic Neocarzinostatin. Origin of the Stabilization of the Chromophore

Masaji Ishiguro,*,† Seiichi Imajo,† and Masahiro Hirama‡

Suntory Institute for Biomedical Research, Shimamoto, Osaka 618, Japan, and Department of Chemistry, Tohoku University, Sendai 980, Japan. *Received January 28, 1991*

A three-dimensional structure of the apoprotein of neocarzinostatin (NCS) was built by using the actinoxanthin (AXN) crystal structure as template, and the subsequent favored-site search for the binding of the fragments (1–4 in Figure 7) of the chromophore (Figure 1) of NCS at the binding cleft led to a reasonable complex structure of apo-NCS and the chromophore (Figures 8 and 9), after refinement of the molecular mechanics program AMBER. The refined three-dimensional structure model of NCS shows the "Y"-shaped cleft of the binding site in which the bicyclic epoxy dienediyne part 4 and its substituents, the naphthoate 3, the amino sugar 2, and cyclic carbonate 1 moieties are nicely fitted. Contacts of the chromophore with the specific amino acid residues in the cleft indicate their contribution to the specific and high affinity binding through ionic interaction, hydrogen bonding, aromatic stacking, and van der Waals contact. Stabilization of the labile chromophore is likely due to the steric hindrance toward the reactive sites such as the C12 position as well as the epoxide, and, more interestingly, the stabilization interaction between the disulfide group (Cys37 and Cys47) and the acetylenic bond is also suggested.

Introduction

Neocarzinostatin (NCS) isolated from the culture filtrates of *Streptomyces carzinostaticus*[1] is a prominent member of the family of macromolecular antitumor antibiotics that include actinoxanthin (AXN)[2] and auromomycin (AUR).[3] NCS consists of an apoprotein composed of 113 amino acids and a non-amino acid chromophore (Figure 1). The isolated chromophore is extremely labile to heat, light, and higher pH (>6) and has been shown to carry the biological activity of the drug by dam-

† Suntory Institute for Biomedical Research.
‡ Tohoku University.

(1) Ishida, N.; Miyazaki, K.; Kumagai, K.; Rikimaru, M. *J. Antibiot.* **1965**, *18*, 68.
(2) Khokhlov, A. S.; Cherches, B. Z.; Reshetov, P. D.; Smirnova, G. M.; Sorokina, I. B.; Koloditskaya, T. A.; Smirnov, V. V.; Navashin, S. M.; Fomina, J. P. *J. Antibiot.* **1969**, *22*, 541.
(3) (a) Chimura, H.; Ishizuka, M.; Hamada, M.; Hori, S.; Kimura, K.; Iwanaga, J.; Takeuchi, T.; Umezawa, H. *J. Antibiot.* **1968**, *21*, 44. (b) Berrman, T. A. *Biochem. Biophys. Res. Commun.* **1978**, *83*, 908.

0022-2623/91/1834-2366$02.50/0

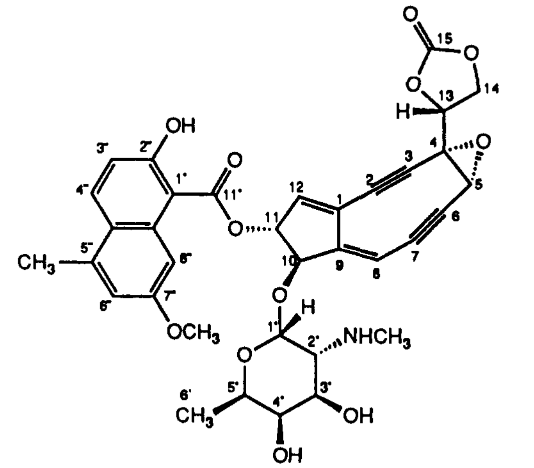

Figure 1. Structure of the NCS chromophore.

aging DNA deoxyribose[4] that might derive from carbon radical formation triggered by nucleophile or hydroperoxy radical.[5,6] The NCS apoprotein (apo-NCS) can bind such a labile chromophore very effectively and specifically ($K_d = 7.0 \times 10^{-6}$),[7] whereas macromomycin (MCR, apoprotein of AUR) or bovine serum albumin cannot do so to such extent.[8] Thus, apo-NCS acts as a specific carrier to protect the chromophore[8,9] and possibly to control its release for interaction with target DNA.[10] A release of the chromophore from NCS has been observed in a substrate-specific manner as well as in a pH-dependent manner.[7] β-Naphthol completely released the chromophore at 3 mM, while only 3% release was detected at the same concentration on α-naphthoic acid. There was also a large difference between D-galactosamine and D-galactose for the chromophore release at 10–500 mM, indicating the importance of the amino group in the *N*-methylfucosamine moiety of the chromophore for the chromophore–apoprotein interaction. Selective oxidation of tryptophane in NCS by *N*-bromosuccinimide (NBS) revealed not only that Trp39 was exposed for chemical modification but that it was not necessary for the chromophore binding whereas Trp83 was resistant to NBS oxidation when the chromophore was bound.[11,12]

The three-dimensional structure of NCS is required in order to understand these observations and to deduce

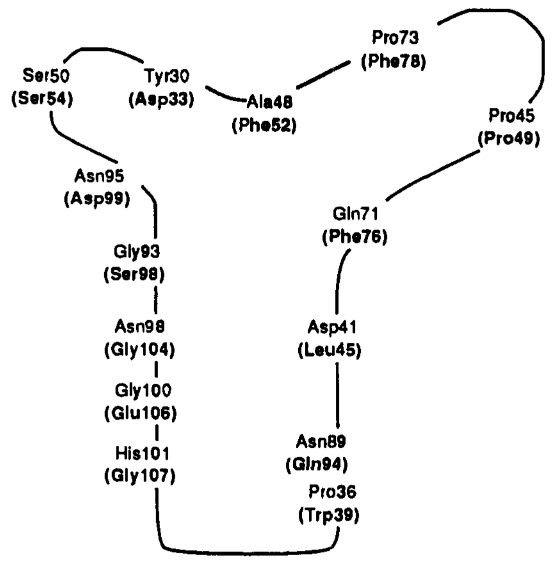

Figure 2. Arrangement of amino acids at the chromophore binding cleft of AXN. The amino acids of apo-NCS corresponding to apo-AXN are shown in parentheses.

```
          S1     10       S2  20           30  S3       40         50
AXN       -APAFSVSPASGASDGQSVSVSVAA--AGETYYIAQCAPVG-GQDACNPA
NCS       AAPTATVTPSSGLSDGTVVKVAGAGLQAGTAYDVGQCAWVDTGVLACNPA
Common     AP   V P SG SDG   V V  A   AG   Y   QCA V   G  ACNPA

          S4        60    S5      70          80         90   S6     100
AXN       TATSFTTDASGAASFSFTVRKSYAGQTPSGTPVGSVDCATDACNLGAGN-
NCS       DFSSVTADADGSASTSLTVRRSFEGFLFDGTRWGTVDCTTAACQVGLSDA
Common       S  T DA  G AS S  TVR  S   G     GT   G VDC T AC   G

                 S7  110
AXN       SGLNLGHVALTFG
NCS       AGNGPEGVAISFN
Common     G      VA
```

Figure 3. Homology alignment between apo-AXN (*Actinomyces globisporus*) and apo-NCS. The standard one-letter code for amino acid residues is used. The β-strands (S1-S7) are underlined and bold italic letters indicate the residues cited in the text.

factors that determine the stabilization of the chromophore by the apoprotein and to design stable analogues of the chromophore. Although the three-dimensional structure of NCS was studied by means of X-ray crystallographic analysis at 3.8-Å resolution,[13] neither the exact structure of the apoprotein nor the interactions between the chromophore and the apoprotein was defined. FT-IR and CD studies as well as X-ray analysis have suggested that the secondary structure of the apoprotein is rich in β-structures.[13,14] The amino acid sequence of apo-NCS was elucidated by the combination of the Edman degradation[15] and FABMS.[15,16] It has been reported that the primary structures of the apoproteins in this family are quite similar. According to the recent results of X-ray crystallographic structure analysis on family proteins,[17] it is reasonable to assume that there should be a high similarity between their tertiary structure as well.

The apoprotein of AXN (apo-AXN, 108 amino acid residues) is the only protein whose three-dimensional

(4) (a) Koide, Y.; Ishii, F.; Hasuda, K.; Koyama, Y.; Edo, K.; Katamine, S.; Kitame, F.; Ishida, N. *J. Antibiot.* **1980**, *33*, 342. (b) Kappen, L. S.; Napier, M. A.; Goldberg, I. H. *Proc. Natl. Acad. Sci. U.S.A.* **1980**, *77*, 1970.
(5) (a) Kappen, L. S.; Goldberg, I. H. *Nucleic Acids Res.* **1985**, *13*, 1637. (b) Chin, D.-H.; Zeng, C.-H.; Costello, C. E.; Goldberg, I. H. *Biochemistry* **1988**, *27*, 8106 and references cited therein. (c) Myers, A. G. *Tetrahedron Lett.* **1987**, *28*, 4493. (d) Myers, A. G.; Proteau, P. J.; Handel, T. M. *J. Am. Chem. Soc.* **1988**, *110*, 7212. (e) Myers, A. G.; Proteau, P. J. *Ibid.* **1989**, *111*, 1146. (f) Tanaka, T.; Fujiwara, K.; Hirama, M. Submitted for publication.
(6) Hirama, M.; Fujiwara, K.; Shigematu, K.; Fukazawa, Y. *J. Am. Chem. Soc.* **1989**, *111*, 4120.
(7) Edo, K.; Saito, K.; A.-Murai, Y.; Mizugaki, M.; Koide, Y.; Ishida, N. *J. Antibiot.* **1988**, *41*, 554. Fujiwara, K.; Kurisaki, A.; Hirama, M. *Tetrahedron Lett.* In press.
(8) Kappen, L. S.; Goldberg, I. H. *Biochemistry* **1980**, *19*, 4786.
(9) Kappen, L. S.; Napier, M. A.; Goldberg, I. H.; Samy, T. S. A. *Biochemistry* **1980**, *19*, 4780.
(10) Povirk, L. F.; Goldberg, I. H. *Biochemistry* **1980**, *19*, 4773.
(11) Edo, K.; Saito, K.; A.-Murai, Y.; Mizugaki, M.; Koide, Y.; Ishida, N. *Abstracts of Papers*, JCU Pharm. Sci. Meeting, Dec. 2–7, 1987, Honolulu, Hawaii, Abstract H 03-W-09. A different selectivity was reported by Samy et al.: see ref 12.
(12) Samy, T. S. A.; Atreyi, M.; Maeda, H.; Meienhofer, J. *Biochemistry* **1974**, *13*, 1007.
(13) Sieker, L. C.; Jensen, L. H.; Samy, T. S. A. *Biochem. Biophys. Res. Commun.* **1976**, *68*, 358. Sieker, L. C. Ph.D. Dissertation (Univ. of Washington, Seattle), 1981.
(14) Saito, K.; Sato, Y.; Edo, K.; A.-Murai, Y.; Koide, Y.; Ishida, N.; Mizugaki, N. *Chem. Pharm. Bull. Jpn.* **1989**, *37*, 3078.
(15) Kuromizu, K.; Tsunasawa, S.; Maeda, H.; Abe, O.; Sakiyama, F. *Arch. Biochem. Biophys.* **1986**, *246*, 199.
(16) Hirayama, K.; Ando, T.; Takahashi, R.; Murai, A. *Bull. Chem. Soc. Jpn.* **1986**, *59*, 1371.
(17) Bajaj, M.; Blundell, T. L. *Annu. Rev. Biophys. Bioeng.* **1984**, *13*, 453.

structure including side chains (2.0-Å resolution) is available from the Brookhaven protein data bank,[18] although the result of the X-ray crystallographic analysis on macromomycin has recently been reported.[19] The crystal structure of apo-AXN is composed to the two structural units of different size, which form a cleft for binding the chromophore. A large, flattened cylinder-shape unit contains two groups of antiparallel β-sheets. The external group consists of three β-strands, S1(Ala3-Val6), S2(Gln16-Ala23), and S5(Ser60-Val65), and another four strands, S3(Thr28-Val37), S4(Ala48-Asp54), S6-(Cys89-Gly94), and S7(His102-Val103), form the internal group that defines the cleft (see Figure 4 for reference). These seven β-strands have a characteristic "Greek key" folding topology that is common to a domain of the immunoglobulin IgG superfamily.[18] The small unit consists of two fragments (Cys34-Pro45 and Thr73-Val79) and a small antiparallel β-sheet (Ser68-Thr73 and Ser81-Asp83). The arrangement of amino acids on the peripheral part of the cleft is shown in Figure 2. Residues of Gly and Ala as well as the disulfide bridge (Cys84 and Cys89) form the bottom of the cleft.[18]

Based on these structural features of apo-AXN, we wish to report a modeling study of the three-dimensional structure of apo-NCS and the NCS complex to explore the binding site of the chromophore and how the apoprotein stabilizes the chromophore.

Alignment

Gibson et al. reported alignment of the amino acid sequence homology between apo-NCS and apo-AXN.[20] However, it has unreasonable insertions such as Gly29 and Ala31 in the β-sheet structure since insertions or deletions are usually found in loop structures. The alignment in Figure 3, obtained by use of the program ALIGN,[21] was adopted for this modeling study. This alignment was in accord with the partial alignment reported recently based on X-ray crystallographic data of apo-AXN and MCR[19] and suggested the following characteristics.

Rather high homology (conservation of 51 out of 113 residues of apo-NCS, 45% amino acid identity) and five insertions (Ala1, Leu26, Gln27, Thr42, and Ala100) are indicated. Occurrence of these insertions at the loop area of apo-AXN suggests high conservation of the major framework of the binding site. The hydrophobic residues essential for the hydrophobic core structure of the large unit such as Phe4 and -51, Ile31, Leu91, and -100, and Ala93 are replaced, except for Ala93, by the smaller hydrophobic residues, Ala5, Val55 and -34 and Pro105, and Leu97, respectively in apo-NCS. These changes will make a closer contact between the external β-sheet (S1, S2, and S5) and cleft-defining internal β-sheet (S3, S4, S6, and S7) in NCS, without a change in the topology of the cleft.

While four (Ala35, Ala42, Val37, and Val82) of the six residues constituting the core of the small unit in apo-AXN are conserved in apo-NCS, the other two (Tyr69 and Val79) are substituted by Phe73 and Trp83, respectively. The tryptophane side chain in apo-NCS, because of its larger size compared to that of valine, will have a different conformational behavior from the valine side chain in apo-AXN.[11]

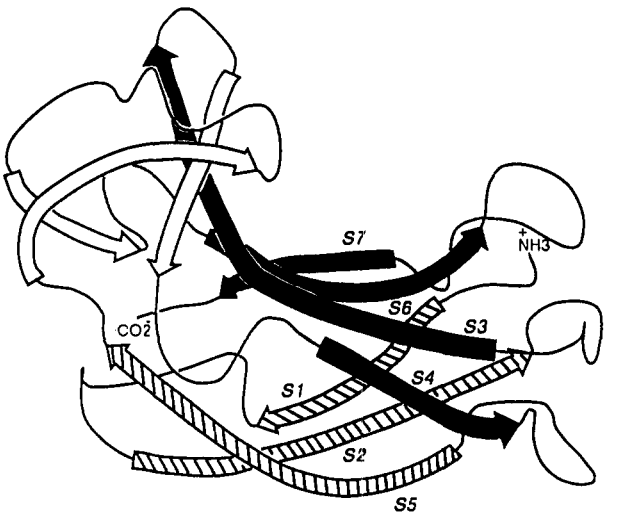

Figure 4. Schematic structure of apo-NCS. Internal sheet (S3,S4,S6,S7) is shown by solid arrows and external sheet (S1,S2,S5) by hatched arrows. Open arrows indicate β-strands found in the small unit.

Eight glycine residues (Gly11, -15, -26, -39, -57, -71, -76, and -97) in the loop regions of apo-AXN are fully conserved in apo-NCS, suggesting an identical structural motif of the folding topology in apo-NCS.[22]

Two basic residues (Arg66 and Lys67) and three acidic residues (Asp14, -54, and -83) on the external surface area of apo-AXN are retained in apo-NCS. Apo-NCS has the additional two basic residues Lys20 and Arg82. They would not be expected to cause a substantial effect on the ionic interactions with the chromophore because they reside at the external surface. While Asp41 in the proximity to the binding cleft of apo-AXN is replaced by Leu45 and apo-NCS, eight acidic residues (Glu74, Glu106, Asp33, Asp41, Asp51,[23] Asp60,[23] Asp79, and Asp99) of apo-NCS have replaced the nonacidic apo-AXN residues. Four of them (Glu106, Asp33, Asp51,[23] and Asp99) are found in the cleft surface, suggesting their contribution to the binding of the chromophore molecule.[23]

Thus, taking account of the recent demonstration on the structural similarity between apo-AXN and MCR,[19] this sequential match of apo-NCS with apo-AXN allows us to utilize the crystal structure of apo-AXN as a template for modeling the tertiary structure of apo-NCS.

Modeling of Apo-NCS

The preliminary three-dimensional structure model of apo-NCS was obtained with the computer graphics program FRODO[24] by substitution of 57 amino acid residues and the insertion of five amino acids (Ala1, Leu26, Gln27, Thr42, and Ala100) into the atomic coordinates of apo-AXN deposited in the Brookhaven protein data bank. For an optimization by the molecular mechanics program AMBER,[25] the steepest descent method was used in order to

(18) (a) Pletnev, V. Z.; Kuzin, A. P.; Trakhanov, S. D.; Kostetsky, P. V. *Biopolymers* **1982**, *21*, 287. (b) Pletnev, V. Z.; Kuzin, A. P.; Malinina, V. Z. *Sov. J. Bioorg. Chem.* **1982**, *8*, 854.

(19) Roey, P. V.; Berrman, T. A. *Proc. Natl. Acad. Sci. U.S.A.* **1989**, *86*, 6587.

(20) Gibson, B. W.; Herlihy, W. C.; Samy, T. S. A.; Hahm, K.-S.; Maeda, H.; Meienhofer, J.; Biemann, K. *J. Biol. Chem.* **1984**, *259*, 10801.

(21) Orcutt, B. C.; Dayhoff, M. O.; George, D. G.; Barker, W. C. ALIGN PIR, version 2.2, National Biomedical Research Foundation, 1984.

(22) Blundell, T.; Lindley, P.; Miller, L.; Moss, D.; Slingsby, C.; Tickle, I.; Turnell, B.; Wistow, G. *Nature* **1981**, *289*, 771.

(23) Assignment of Asp or Asn residues is reversed at 48, 51, 60, 87, and 103 between the two reports cited in refs 16 and 20. However, it may not affect the structure modeling, because most of them are far from the cleft surface.

(24) Jones, T. A. *Methods Enzymol.* **1985**, *115*, 157; *J. Appl. Cryst.* **1978**, *11*, 268.

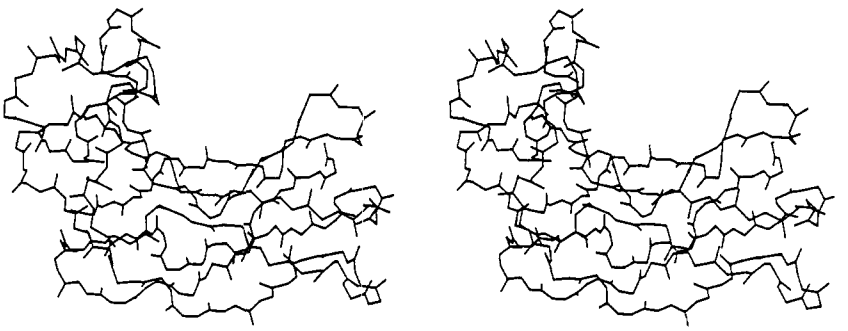

Figure 5. Stereoview of a main-chain structure of the 3D model of apo-NCS.

avoid the generation of an overly compact structure by energy minimization[26] since minimization of the structure inside a box of water molecules still gave an overly compact structure. The preliminary structure was optimized by this method until the maximum gradient became less than 0.1 kcal/mol/Å. The refined apo-NCS model thus obtained is very similar to the structure of apo-AXN as expected (Figures 4 and 5).[19] A Y-shaped cleft similar to apo-AXN is easily recognizable, indicating that the chromophore-binding site is composed of at least three characteristic pockets as shown in Figure 2. The large pocket surrounded by Leu45, Trp39, Gln94, Gly107, Glu106, Gly104, and Ser98 shows a smoother bottom surface than that in apo-AXN, since six Cα protons of Val34, Gly35, and Gln36 (S3) and Val95, Gly96, and Leu97(S6) in the antiparallel β-sheets form the bottom surface in NCS while the methyl group of Ala32 in AXN (Gly35 in NCS) sticks out from the bottom surface. The small pocket composed of Ser54, Asp33, Asp99 is rather shallow and hydrophilic. The medium pocket is lined by Phe76 and Phe78, which are quite different from the corresponding apo-AXN residues. Pro49 and Ser54 in apo-NCS are the only residues conserved in this peripheral part. These observations suggest that the specific side chains in the binding pockets may be responsible for the chromophore binding selectivity.[8] In other words, chromophores bound to the analogous apoproteins would have a different structure or at least different substituents.[18] This can be supported by the result of recent work on the X-ray crystallographic analysis of macromomycin.[19]

Binding-Site Exploration

Although the NOE experiment of the thiol-reacted molecule derived from the chromophore has been done in its solution,[5e] the apoprotein-bound conformation, which may be different from the conformation of the thiol-reacted molecule, is not known. It would be difficult to elucidate the apoprotein-bound structure by a conformational search of all possible conformations for the chromophore without any structural constraint. Analysis of the binding sites for the substituents (1–3) attached to the bicyclic dienediyne carbocyclic core (carbocyclic core 4) will afford the necessary constraints for a search of the apoprotein-bound conformation of the chromophore. Thus, definition of the binding site for the substituents and the subsequent connection of these fragments (1–4) would give rise to the apoprotein-bound conformation of the chromophore after the refinement of the structure in the presence of the apoprotein.[27]

The experiments that β-naphthol and D-galactosamine displace the chromophore at the binding site but not α-naphthoic acid and D-galactose indicate that amino group of the sugar moiety and the hydroxy group of the naphthoate moiety play an important role for molecular recognition with specific amino acid residues at the binding cleft. The program, GRID, reported by Goodford[28,29] is a suitable tool for exploring specific sites at the surface of a binding cleft where these functional groups interact favorably. The chromophore has carbonate 1 and epoxide groups at either end of the carbocyclic core 4 as functional groups that will be expected to participate in a specific recognition between the apoprotein and the chromophore. Before exploring specific sites for these four functional groups, sites specific for water examined since protein molecules often have binding sites for water molecules at substrate recognition sites that often play a crucial role in the structural stability and the catalytic activity of proteins.[29] The GRID surface was calculated at the area, 22 × 24 Å widths and 21 Å depth, that covers the whole binding cleft.

Water-Specific Sites. Two water binding sites in the chromophore binding cleft were found at −9.0 kcal/mol by using the water probe in a GRID calculation.[29] One of these specific sites was located at the bottom of the medium pocket surrounded by the carbonyls of Asn48 and Gln36 as well as the amide hydrogens of Gln36 and Phe52. A water molecule at this site should have a common and specific role in ligand binding or in the stability of proteins of this family, since this specific site was also suggested in apo-AXN by a GRID search. Furthermore, the presence of a specific water molecule found at the corresponding site in MCR by X-ray crystallographic analysis[19] confirms its important role in this protein family. The other site specific for water was found at the edge of the larger pocket, and this water molecule is likely to form hydrogen bonds with the carbonyls of Cys37 and Ala92 and with the Trp39 amide hydrogen. After placing two water molecules at these sites where the water molecules form hydrogen bonds as mentioned above, the resulting apo-NCS structure was again refined by AMBER[25] until the maximum gradient became less than 0.1 kcal/mol/Å by the conjugate gradient method with an assumption that favored surfaces for the probes would not vanish completely. In fact, similar surfaces for the probes were found at the binding cleft in both refined or unrefined models, although the refined

(25) Singh, U. C.; Weiner, P, K.; Caldwell, J. W.; Kollman, P. A. AMBER UCSF, version 3.0, Dept. of Pharm. Chem., University of San Francisco, 1986. Weiner, S. J.; Kollman, P. A.; Nguyen, D. T.; Case, D. A. *J. Comput. Chem.* **1986**, *7*, 230. Weiner, S. J.; Kollman, P. A.; Case, D. A.; Singh, U. C.; Ghio, C.; Alagona, G.; Profeta, S. Jr.; Weiner, P. K. *J. Am. Chem. Soc.* **1984**, *106*, 765.

(26) Gilson, M. K.; Honig, B. *Proteins: Structure, Function and Genetics* **1988**, *4*, 17.

(27) DesJarlais, R. L.; Sheridan, R. P.; Dixon, J. S.; Kuntz, I. D.; Venkataraghaven, R. *J. Med. Chem.* **1986**, *29*, 2149.

(28) Goodford, P. J. *J. Med. Chem.* **1985**, *28*, 849. GRIN, GRID, and GRAB, version 6.0, Molecular Discovery Ltd., 1989.

(29) Reynolds, C. A.; Wada, R. C.; Goodford, P. J. *J. Mol. Graphics* **1989**, *7*, 103.

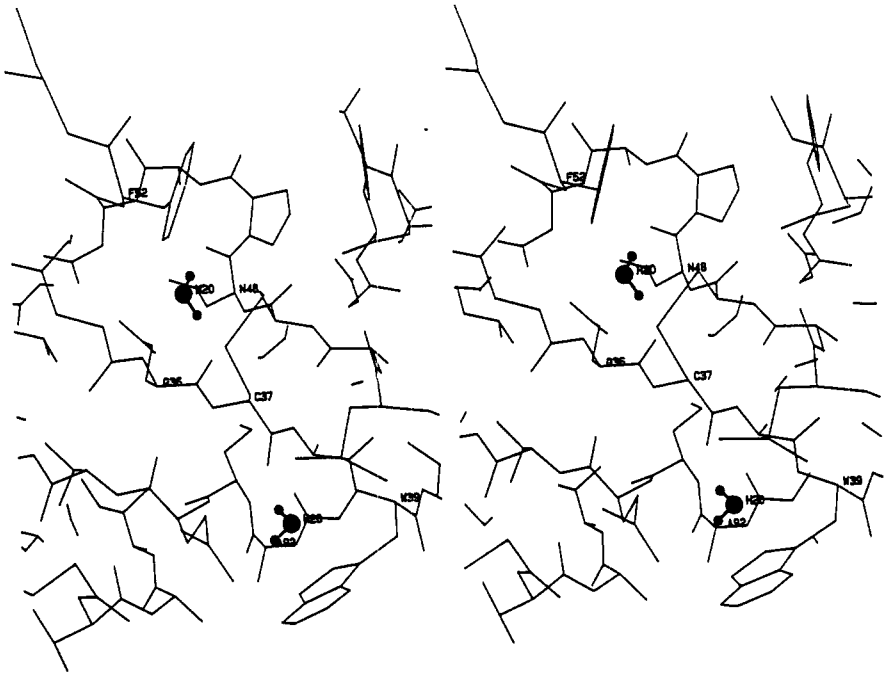

Figure 6. Stereoview of a binding cleft of apo-NCS with two water molecules shown by ball and stick.

protein model was slightly more compact than the initial structure. The refined apo-NCS structure with two specific water molecules (Figure 6) was then used as the model for the binding-site exploration.

Favored Sites for Amino, Naphthol, Carbonyl, and Epoxy Groups. Potential energy calculations using a secondary ammonium probe showed the most favored surface at −17.0 kcal/mol. This specific site for the *N*-methylammonium group in *N*-methylfucosamine **2** is formed especially by Asp33, Asp99, and Ser54 in the small pocket (Figure 2), indicating an ionic interaction[7] among these functional groups. Taking into account the direction of the α-glycosidic linkage[30] with the carbocyclic core **4** and the specific site for the amino group, *N*-methylfucosamine **2** was unambiguously located at this small pocket, which was of a size for only a monomeric sugar.

The binding surface for a naphthol moiety **3** was explored by use of the aromatic carbon probe and the phenolic hydroxyl probe. The favored site for phenolic hydroxyl was found at the bottom of the medium pocket, where the preferred binding site of aromatic carbon was also found at −4.0 kcal/mol. This finding strongly indicated that the naphthol moiety would occupy the medium pocket. Since this pocket is formed by Pro49, Phe52, Phe76, and Phe78, it seems to be reasonable as the aromatic binding site (Figure 2). With the guidance of this favored surface for the phenolic hydroxy group and with the direction of its ester linkage, the naphthoate group **3**, which initially had an intramolecular hydrogen bond between the hydroxy and the carbonyl groups, was adapted to the medium pocket.

Characteristic carbonyl-favored sites were found specifically around Ser98 at −4.0 kcal/mol. This suggests a participation of Ser98 in the recognition of carbonate group **1** at the large pocket. In addition, the hydrophobic side chain of Leu45 was found at a van der Waals contact distance with the carbonate C14 methylene group. Thus, it was concluded that the carbonate group **1** would exist at this site in the large pocket. Guided by these two van der Waals contacts, the carbonate group **1** could find a suitable site for binding.

Since GRID has no epoxide probe,[29] the ether probe was used as a substitute for the epoxide group. A specific surface was obtained at −3.0 kcal/mol. This surface is in the bottom of the large pocket and consists of Gly35, Gly96, and Gly107. The oxygen atom of the epoxide could be localized at the center of this surface.

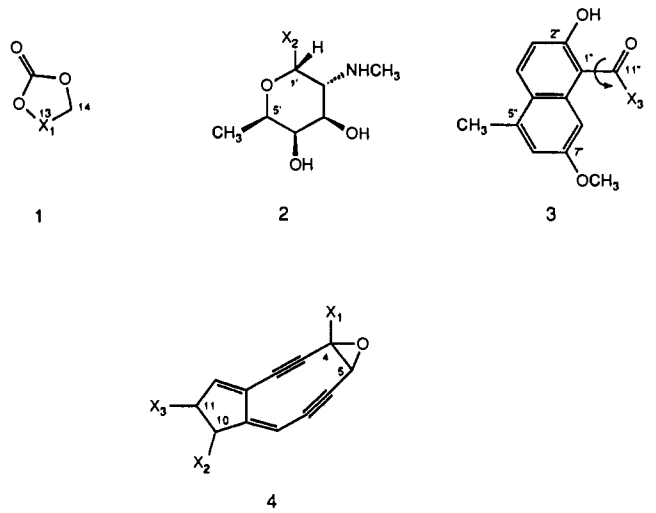

Figure 7. Three substituents (**1**, **2** and **3**) and the carbocyclic core **4** of the NCS chromophore with a 4,5-epoxide.

Model Building of the NCS Complex Structure

After defining four specific sites for the substituents of the chromophore in the cleft, these have to be connected to the carbocyclic core **4** in order to build a complete structure of the chromophore and a model of NCS. The connection of the carbocyclic core **4** and the sbustituents **1**–**3** was examined without use of the data on the configuration at C-4, -5, -10, -11, and -13 except for the trans stereochemistry between substituents at C10 and C11.[30] Thus, the molecules corresponding to the three substituents (**1**, $X_1 = CH_2$; **2**, X_2 = OMe; **3**, X_3 = OMe) shown in Figure 7 could be placed at the proper position. Then, the

(30) Edo, K.; Mizugaki, M.; Koide, Y.; Seto, H.; Furihata, K.; Otake, N.; Ishida, N. *Tetrahedron Lett.* **1985**, *26*, 331. When this modeling study was started, only partial stereochemistry reported in ref 33 was known.

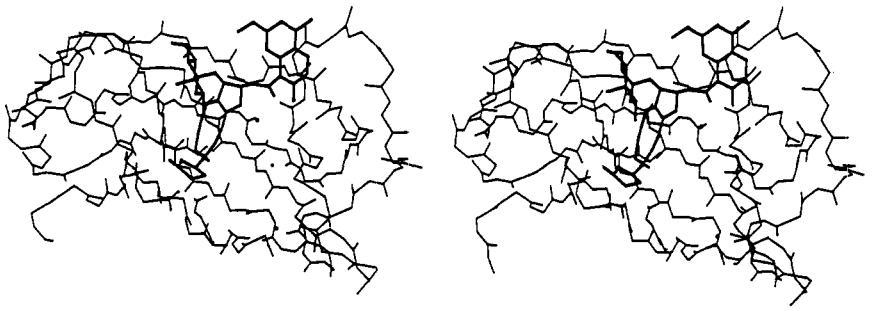

Figure 8. Stereoview of the refined NCS model. Apo-NCS (thin line) is shown by its main chain only. The hydrogens of the chromophore (thick line) are neglected.

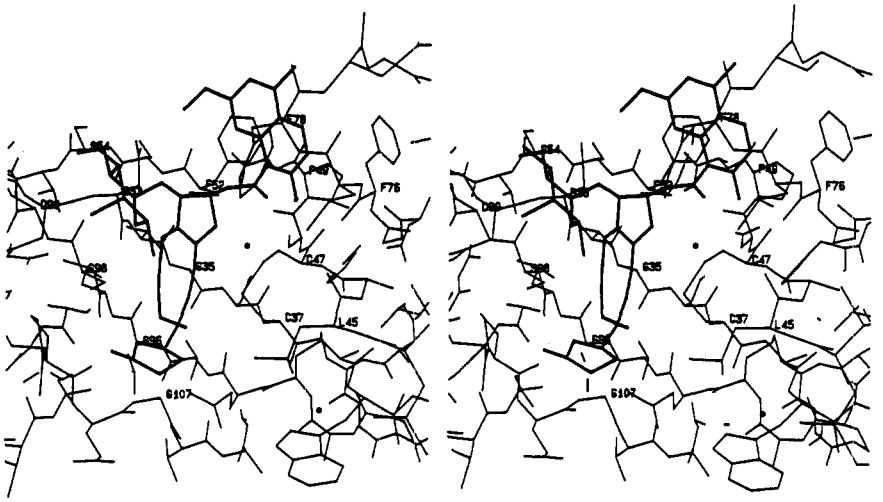

Figure 9. Stereoview of NCS chromophore at the binding cleft of apo-NCS. The Y-shaped binding site is shown with side chains and the chromophore by the thick line.

4,5-epoxy carbocyclic core (**4**, $X_1 = CH_3$, $X_2 = X_3 = OH$), which was generated and optimized by MM2 in MACROMODEL,[31] was put in the large pocket and the most suitable position to properly connect to the three substituents **1–3** was investigated as follows. Taking account of the trans stereochemistry between substituents at C10 and C11,[30] four possible stereosiomers for structure **4** were generated and examined by root-mean-square (rms) fitting calculations between the four atoms [i.e., epoxide oxygen, X_1 (= C) in **1**, X_2 (= O) in **2**, and X_3 (= O) in **3**] at the binding cleft and the corresponding atoms in structure **4** (4*R*,5*S* or 4*S*,5*R* and 10*R*,11*R* or 10*S*,11*S*). Since the torsional angle C1″–C11″ of molecule **3** could not be restricted to a particular one, 36 rotational conformers were generated by the rotation of the bond every 10° and rms fitting calculations were then taken with each conformer. The best fit value ($r = 0.76$) was obtained for the structure having a 4*R*,5*S*,10*R*,11*R* configuration while the minimum rms values of 1.51, 1.66, and 1.79 were obtained for the isomers having 4*R*,5*S*,10*S*,11*S*,4*S*,5*R*,10*S*,11*S*, and 4*S*,5*R*,10*R*,11*R*, respectively. Therefore, the most probable stereochemistry of the chromophore could be deduced to be 4*R*,5*S*,10*R*,11*R*. Connection of C4 in the core **4** and C13 in the carbonate group **1** consequently defines the configuration of C13 as *R* (Figure 1). These results are in good agreement with Myers' stereochemical assignment based on an NMR study.[5e]

The unrefined chromophore structure thus obtained had a few improper bond lengths and bond angles at the connecting sites. The whole structure of NCS including the apoprotein, two water molecules, and the unrefined chromophore was then subjected to optimization by AMBER until the maximum gradient became less than 0.1 kcal/mol/Å by the conjugate gradient method.[32]

Table I. Selected Atomic Distances between the Chromophore and the Apoprotein in the NCS Model

chromophore		apoprotein	distance (Å)
acetylene	C2	Cys37 S_γ	3.46
		Cys47 S_γ	3.92
		Ser98 C_β	4.14
	C3	Cys37 S_γ	3.39
		Cys47 S_γ	4.41
		Ser98 C_β	3.99
	C6	Cys37 S_γ	4.43
		Cys47 S_γ	5.70
		Ser98 C_β	3.61
	C7	Cys37 S_γ	4.62
		Cys47 S_γ	5.50
		Ser98 C_β	3.66
methylene	C14	Leu45 C_γ	4.76
		C_δ	3.37
carbonyl	O15	Ser98 O_γ	2.85
amino	N2′	Asp33 O_δ	2.62
		Asp99 O_δ	3.77
hydroxy	O3′	Asp99 O_δ	3.77
methyl	O3′	Phe78 C_γ	6.01
		C_δ	4.71
		C_ϵ	4.33
naphthalene	C9″	Phe52 C_γ	3.70
	C10″	C_ζ	3.25

(31) MACROMODEL, version 1.1, Columbia University, 1986.

(32) Charges for the chromophore were obtained from MNDO calculation of an optimized structure of the chromophore by MM2. Bond and angle parameters were set from the optimized structure and parameters for torison were approximated mainly from those of the corresponding second and third atoms used in AMBER and MM2 in MACROMODEL. The harmonic force constants were adjusted to give a proper structure by comparison with the structure optimized by MM2.

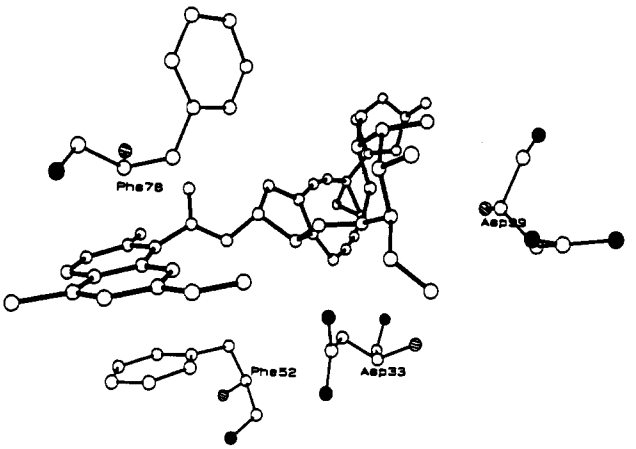

Figure 10. Specific interaction of the *N*-methylfucosamine and naphthyl group of the chromophore (thick line) at the binding cleft by ionic (Asp33) and hydrogen bonds (Asp99) and aromatic stacking (Phe52). Closed and hatched circles indicate oxygen and nitrogen atoms of amino acid residues, respectively.

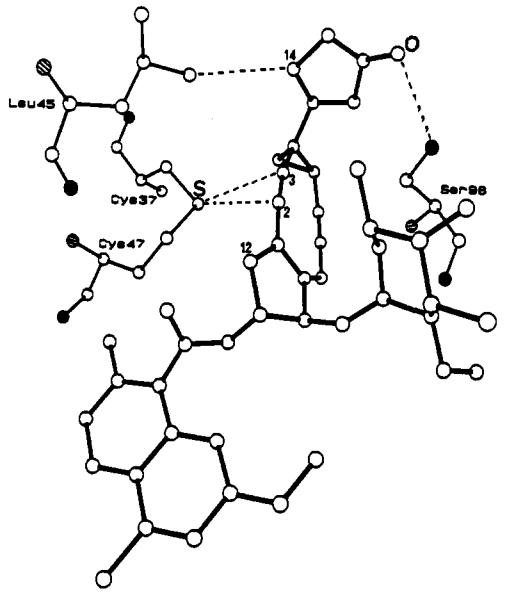

Figure 11. Specific binding mode of carbonate group at the binding cleft by hydrogen bond (Ser98) and the characteristic van der Waals contact of the sulfur group of Cys37 with the acetylenic C2–C3 bond. Closed and hatched circles indicate oxygen and nitrogen atoms of amino acid residues, respectively.

The NCS Structure

The optimized structure of the NCS complex obtained is shown in Figures 8 and 9. Main chain atoms were retained almost at the original positions compared with model apo-NCS (Figure 5). Only the conformations of some side chains in the binding site were changed. The characteristic close contacts of protein residues with the chromophore are summarized in Table I and their putative interactions are as follows. The amino group and 3′-hydroxy group of the *N*-methylfucosamine moiety **2** have specific interactions through a hydrogen bond with Asp33 and Asp99 in the small pocket (Figure 10). The methyl group (C6′) of the sugar **2** is facing over the 5-membered ring of the carbocyclic core **4** of the chromophore and most likely covers its C12 position, which is susceptible to nucleophilic[5c] and radical (oxygen)[6] attack. The Phe78 residue, (Figure 10) is located approximately at a van der Waals distance from this methyl group, covering also the C12 position (see Table I). The carbonate carbonyl group appears to be interacting with Ser98 by hydrogen bonding, while the Leu45 side chain is located in good van der Waals contact with the C14-methyene group of the carbonate **1** (Figure 11). The epoxide group seems to enjoy a good fit in the hydrophobic pocket, lacking any interactions that accelerate ring opening. The carbocyclic core **4** of the chromophore sits diagonally in the center of the large pocket, facing the C6–C7 acetylenic bond to the bottom of the cleft, which is consisted of α-protons of Val34, Gly35, Gly96, and Leu97 (Figures 8 and 9). Since the bottom of the cleft is smooth and hydrophobic, this hydrophobic interaction between ligand and protein must be very favorable. The other acetylenic bond (C2–C3) experiences close van der Waals contact by lying close to the Cβ-methylene of Ser98 and the sulfur atom of Cys37, which forms a disulfide bond with Cys47 (Figure 11 and Table I). The naphthol group **3** occupies the medium pocket, forming a typical aromatic stacking interaction with Phe52 (Figure 10). It is remarkable that the phenolic hydroxy group at C2″ showed an intermolecular hydrogen bond with the carbonyl oxygen of Phe76 in spite of a starting structure, which had an intramolecular hydrogen bond with the ortho carbonyl group. Inspection of the Cambridge Crystallographic Database revealed that 6-substitued 2-hydroxybenzoate derivatives have no intramolecular hydrogen bonds but show intermolecular hydrogen bonds in crystals due to steric reasons. This result is also in accord with the competitive displacement of the chromophore by β-naphthol mentioned earlier.[7] Thus, all parts of the NCS chromophore seem to show very favorable interactions with the apoprotein residues in the cleft.

It is reasonable to compare the putative apoprotein-bound conformation described above with the other energetically favored structures obtained by the full conformation search of the chromophore generated by the rotation of the bonds C4–C13, C10–O10, O10–C1′, C11–O11, O11–C11″, and C11″–C1″ (see Figure 1) in 30° intervals using MM2 parameters. Through this search, 64 distinguished conformers were obtained within 5 kcal/mol from the most stable conformer. The putative apoprotein-bound conformation was found to be very similar to the conformation that is 1.5 kcal/mol higher in enery than the lowest energy conformer (Figure 12). A comparison with the DNA-bound conformation and/or the structure in a solution whose structures have not yet been

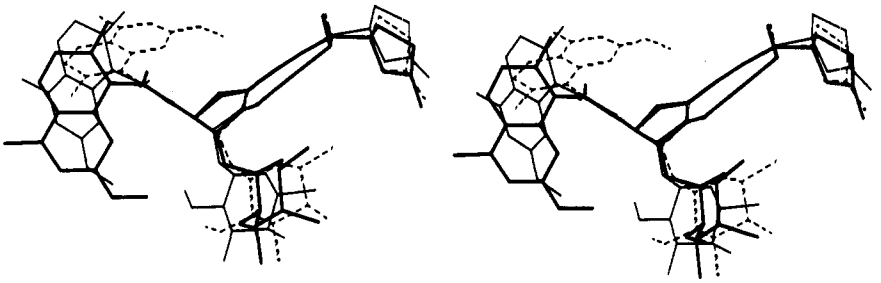

Figure 12. Similarity of the putative apoprotein-bound conformation (heavy lines) to the conformation found by the full conformation search (fine lines). The most stable conformation is shown by dashed lines.

elucidated exactly will be the subject of future studies.

Edo et al. reported that Trp83 must exist at the binding site because of its resistance against oxidation in the chromophore-bound structure.[11,12] However, in the model, Trp83 is located far from the binding site and contributes to the formation of the hydrophobic core in the small unit, whereas Trp39 is close to the binding site of the carbonate group of the chromophore. Therefore, it is not unlikely that upon binding of the chromophore the protein structure becomes more rigid and so does the side chain of Trp83, which is kept buried inside. This also suggests a rigid conformation of the chromophore at the binding cleft.

Conclusion

The significant increase of the thermal, chemical, and photochemical stability of the chromophore in the complexed form[8,9] is likely a result of the following interactions: (1) the hydrophobic environment of the epoxide and the unsaturated bonds; (2) steric coverage of the active reaction site (C12) with Phe78 and the methyl group (C6') of the amino sugar moiety; (3) stabilization of a rigid conformation of the chromophore by a network of hydrogen bonds and hydrophobic interactions at the binding cleft; and (4) more interestingly, the possible interaction between the sulfur atom of Cys37 and the C2-C3 acetylenic bond. While the last interaction awaits experimental verification, the close intermolecular contact reminds us of the intramolecular trisulfide bond of the structurally related potent antitumor antibiotics calicheamicins[33] and esperamicins.[34] A possible stabilizing interaction of the trisulfide or disulfide unit is experimentally and theoretically under investigation in these laboratories.

Acknowledgment. We thank Profs. Michinao Mizugaki and Kiyoto Edo, Tohoku University Hospital, for helpful discussions.

Registry No. Neocarnostatin apoprotein, 101359-79-9; neocarzinostatin chromophore, 81604-85-5.

Supplementary Material Available: Tables of atomic coordinates for the NCS chromophore and for Cα of apo-NCS (4 pages). Ordering information is given on any current masthead page.

(33) (a) Zein, N.; Sinha, A. M.; McGahren, W. J.; Ellestad, G. A. *Science (Washington, D.C.)* 1988, *240*, 1198 and references therein. (b) Ellestad, G. A.; Hamann, P. R.; Zein, N.; Morton, G. O.; Siegel, M. M.; Pastel, M.; Borders, D. B.; McGahren, W. J. *Tetrahedron Lett.* 1989, *30*, 3033.

(34) Long, B. H.; Golik, J.; Forenza, S.; Ward, B.; Rehfuss, R.; Dabrowaik, J. C.; Catino, J. J.; Musial, S. T.; Brookshire, K. W.; Doyle, T. W. *Proc. Natl. Acad. Sci. U.S.A* 1989, *86*, 2 and references cited therein.

Synthesis and Antitumor Evaluations of Symmetrically and Unsymmetrically Substituted 1,4-Bis[(aminoalkyl)amino]anthracene-9,10-diones and 1,4-Bis[(aminoalkyl)amino]-5,8-dihydroxyanthracene-9,10-diones

A. Paul Krapcho,*,† Zelleka Getahun,† Kenneth L. Avery, Jr.,† Kevin J. Vargas,† and Miles P. Hacker‡

Departments of Chemistry and Pharmacology, University of Vermont, Burlington, Vermont 05405

Silvano Spinelli, Gabriella Pezzoni, and Carla Manzotti

Boehringer Mannheim Italia SPA, Monza, Italy. *Received January 7, 1991*

The ipso bis displacements of fluoride from 1,4-difluoroanthracene-9,10-dione (3) and 1,4-difluoro-5,8-dihydroxyanthracene-9,10-dione (4) by excess of a diamine (or a monoamine) in pyridine at room temperature lead to the symmetrically substituted 1,4-bis-substituted analogues 5 and 6, respectively. The ipso monodisplacements of fluoride from 3 and 4 can be accomplished by treatment with less than 1 molar equiv of a diamine (or a monoamine) to yield 7 and 8, respectively. Treatment of 7 or 8 with a different diamine leads to the unsymmetrically substituted 1,4-bis[(aminoalkyl)amino]anthracene-9,10-diones 9 and 10, respectively. Many of the synthetic unsymmetrical analogues have been evaluated for their antitumor activity against L1210 in vitro and in vivo. Cross resistance of analogue 10a with mitoxantrone (2) and doxorubicin was evaluated against MDR lines in vitro against human colon carcinoma LOVO and its subline resistant to DOXO (LOVO/DOXO). Potential mechanisms for the observed cytotoxicity are presented and discussed.

The discovery of the antitumor activity of 1,4-bis[(aminoalkyl)amino]anthracene-9,10-diones such as ametantrone (1) and mitoxantrone (2)[1-4] has led to numerous physicochemical and pharmacological studies on the tumoricidal mechanisms of these chemotypes.[5]

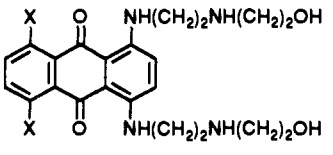

1, X = H
2, X = OH

Mitoxantrone (2) is an important new drug with demonstrated clinical efficacy in the treatment of leukemia,

† Department of Chemistry.
‡ Department of Pharmacology.

(1) (a) Cheng, C. C.; Zee-Cheng, R. K. Y. *Prog. Med. Chem.* 1983, *20*, 83 and references cited therein. (b) Zee-Cheng, R. K. Y.; Cheng, C. C. *Drugs Future* 1983, *8*, 229. (c) Zee-Cheng, R. K. Y.; Podrebarac, E. G.; Menon, C. S.; Cheng, C. C. *J. Med. Chem.* 1979, *22*, 501.

(2) (a) Zee-Cheng, R. K. Y.; Cheng, C. C. *J. Med. Chem.* 1978, *21*, 291. (b) Murdock, K. C.; Child, R. G.; Fabio, P. F.; Angier, R. B.; Wallace, R. E.; Durr, F. E.; Citarella, R. V. *J. Med. Chem.* 1979, *22*, 1024.

(3) Krapcho, A. P.; Shaw, K. J.; Landi, J. J., Jr.; Phinney, D. G.; Hacker, M. P.; McCormack, J. J. *J. Med. Chem.* 1986, *29*, 1370.

(4) (a) Stefanska, B.; Dzieduszycka, M.; Martelli, S.; Borowski, E. *J. Med. Chem.* 1989, *32*, 1724. (b) Dzieduszycka, M.; Stefanska, B.; Kolodzieczyk, P.; Borowski, E.; Martelli, S. *Farmaco Ed. Sci.* 1987, *42*, 219.

0022-2623/91/1834-2373$02.50/0